Radio Science, Volume ???, Number , Pages 1–15,

The numerical calibration of the STEREO/SWAVES monopole antennas

Oswald, T.H.,[1] H.O. Rucker,[1] W. Macher,[1] G. Fischer,[1] U. Taubenschuss,[1] M.L. Kaiser,[2] K. Goetz,[3] J.L. Bougeret,[4] and A. Lecacheux[4]

STEREO is a space mission conducted by NASA, to be launched in April 2006. It consists of two spacecraft which will follow a sun centered trajectory at approximately one AU, one ahead, the other behind earth, slowly drifting apart. The SWAVES experiments onboard the two STEREO spacecraft will perform measurements of the non-thermal radio spectrum from 10 kHz up to about 16 MHz and at 2 frequencies just above 30 MHz. For this purpose 3 orthogonal, six meter long monopole stacer antennas and a set of receivers are used, thereby enabling direction finding, i.e. the determination of the direction of arrival and the polarization state of the observed radio waves. This direction finding capability, which requires an exact knowledge of the antenna properties, in combination with the two spacecraft, opens the possibility to locate the radio sources by means of triangulation. Numerical wire-grid simulations of the antenna system have been performed to determine the effective length vectors of the antennas, which are the most suitable representation of the receiving properties of antennas. The results are presented in this paper, with a view to the intended direction finding applications.

1. Introduction

The existence of two spatially separated spacecraft observing radiation of the same source simultaneously, in combination with direction finding capabilities, enables a new type of observation. The location of the radio sources can be pinpointed via triangulation and its evolution can be tracked from the surface of the sun, to earth's orbit and beyond.

Direction finding is the procedure of finding the direction of the incident wave as well as the Stokes parameters, which define the state of its polarization, from the measured observables. The measured observables are the auto- and cross-correlation parameters of the antennas. For three axes stabilized spacecraft with three antennas, like the STEREO spacecraft, there exist equations which can be used to perform this task (*Cecconi and Zarka* [2005]). But

[1]Space Research Institute, Austrian Academy of Sciences, Graz, Austria.
[2]NASA/GSFC, Greenbelt, MD, USA.
[3]University of Minnesota, USA.
[4]Observatoire de Paris-Meudon, France

0048-6604/06/$11.00

to succeed, it is of vital importance to know the reception properties of the antennas to a high degree of accuracy. A very elegant and concise method of describing the receiving property of an antenna is the effective length vector, which is a generalization of the well known effective height. Four known methods exist to determine the effective length vector of a spacecraft antenna:

1. Numerical wire grid modelling
2. Experimental rheometry
3. The EMC chamber
4. Inflight calibration

The effective length vectors and impedances of the STEREO/WAVES antennas were computed by a numerical method, using the open source ASAP software and several routines developed by us. In this paper we shall give a short description of direction finding, effective length vectors and the numerical method of finding them. Then we shall proceed to show and discuss the results of the numerical computation.

2. Antennas on spacecraft, the Stokes parameters and the effective length vectors

There are two types of antennas used on most spacecraft. One type is used for communication. Normally parabolic antennas are well suited for this task. The other type of antennas to be discussed here, is used to receive radiation from natural sources. Simple antennas, like monopole, dipole or loop antennas are used in this case. The STEREO/WAVES experiment works with three mutually orthogonal stacer monopole antennas. They are connected to a receiver which operates in a frequency range of 10 kHz up to about 16 MHz. Two receiver modi exist. The direction finding mode, where all auto- and cross-correlation-parameters are measured and recorded and a mode where two of the three antennas are combined to give a dipole.

The auto- and cross-correlation parameters for two antennas, say i and j, are defined as the average product of the voltage induced on one antenna with the complex conjugate of the voltage induced on the same, or the other antenna, respectively. So for two antennas i and j they are

$\langle V_i V_i^* \rangle$
$\langle V_i V_i^* \rangle$
$\Re \langle V_i V_j^* \rangle$
$\Im \langle V_i V_j^* \rangle$

and the time average can be understood as

$$\langle CC^* \rangle = \frac{1}{T} \int_0^T CC^* dt \tag{1}$$

where the integration time T must be long in relation to the period of the received radiation.

The Stokes parameters S_0 to S_3 are one of several possibilities of representing the state of polarization of the received wave. The normalized parameters $\hat{I}$, $\hat{Q}$, $\hat{U}$ and $\hat{V}$ can be written as

$$\frac{S_0}{2\eta_0} = \hat{I} = \frac{\langle E_x^2 \rangle + \langle E_y^2 \rangle}{2\eta_0} \tag{2}$$

$$\frac{S_1}{S_0} = \hat{Q} = \frac{\langle E_x^2 \rangle - \langle E_y^2 \rangle}{\langle E_x^2 \rangle + \langle E_y^2 \rangle} \tag{3}$$

$$\frac{S_2}{S_0} = \hat{U} = \frac{\langle 2E_x E_y \cos\delta \rangle}{\langle E_x^2 \rangle + \langle E_y^2 \rangle} \tag{4}$$

$$\frac{S_3}{S_0} = \hat{V} = \frac{\langle 2E_x E_y \sin\delta \rangle}{\langle E_x^2 \rangle + \langle E_y^2 \rangle} \tag{5}$$

where E_x and E_y are the components of the electric field in the direction of the x- and y-axes of the wave frame, given that the wave vector $\mathbf{k}$ points along the z-axis. η_0 is the impedance of free space and δ the phase shift between the components of the electric field in the x and y direction.

The voltage induced on an antenna is the inner product of the vector describing the antenna, with the sum of the electric field vectors of all incident waves at its phase center. It is not the geometrical length vector of the antenna, but the effective length vector, which is to be used in this equation.

$$V = \sum_w \mathbf{h}_{eff,w} \cdot \mathbf{E}_w \tag{6}$$

The sum is over all different incident waves, weather electromagnetic or electrostatic in nature. It is a well known result of electrodynamics, that the effective length of an ideal short dipole is half the length of the physical antenna. In case of a space-

craft the difference is even more pronounced and the effective length vector is not only differing in length, but also in direction.

The reason is, that the surface of the whole spacecraft is made of a conducting material, such that it acts itself like an antenna. So one is not dealing with a simple monopole, but with an antenna of very complicated structure. Fortunately, at low frequency, the so called quasistatic range, the behavior of the antenna can be represented by a single effective length vector.

At high frequencies, where the wavelength of the incident wave can not be regarded as large in relation to the spacecraft dimensions, the effective lengths vector depends on frequency and direction of the radiation and the imaginary part becomes large. Then, this concept is not useable any more.

3. Direction finding

When the coordinate frame shown in figure 1 is used, the following relationship between the correlation parameters for antennas i and j on one side and the coordinates and Stokes parameters on the other side can be found (see *Oswald* [2005]):

$$\begin{aligned}\langle V_i V_i^* \rangle \;=\; & \hat{S}\eta_0 h_{eff,i}^2[(\hat{Q}+1)(\sin^2\theta\cos^2\alpha_i - \\ & -\frac{1}{2}\sin(2\alpha_i)\sin(2\theta)\cos^2(\varphi-\Omega_i) + \\ & +\sin^2\alpha_i\cos^2\theta\cos^2(\varphi-\Omega_i)) + \\ & +(1-\hat{Q})\sin^2\alpha_i\sin^2(\varphi-\Omega_i) + \\ & +\hat{U}(-\sin\theta\sin 2\alpha_i\sin(\varphi-\Omega_i) + \\ & +\sin^2\alpha_i\cos\theta sin(2\varphi-2\Omega_i))] \qquad (7)\end{aligned}$$

$$\begin{aligned}\Re\left\langle V_i V_j^* \right\rangle \;=\; & \hat{S}\eta_0 h_{eff,i} h_{eff,j}[(\hat{Q}+1)(\sin^2\theta\cos\alpha_i\cos\alpha_j - \\ & -\frac{1}{2}\sin(2\theta)(\sin\alpha_j\cos\alpha_i\cos(\varphi-\Omega_j) + \\ & +\sin\alpha_i\cos\alpha_j\cos(\varphi-\Omega_i)) + \\ & +\sin\alpha_i\sin\alpha_j\cos^2\theta\cos(\varphi-\Omega_i)\cos(\varphi-\Omega_j)) + \\ & +(1-\hat{Q})\sin\alpha_i\sin\alpha_j\sin(\varphi-\Omega_i)\sin(\varphi-\Omega_j) - \\ & -\hat{U}(\sin\theta(\sin\alpha_i\cos\alpha_j\sin(\varphi-\Omega_i) + \\ & +\sin\alpha_j\cos\alpha_i\sin(\varphi-\Omega_j)) - \\ & -\cos\theta\sin\alpha_i\sin\alpha_j(\sin(\varphi-\Omega_j)\cos(\varphi-\Omega_i) + \\ & +\sin(\varphi-\Omega_i)\cos(\varphi-\Omega_j)))] \qquad (8)\end{aligned}$$

$$\begin{aligned}\Im\left\langle V_i V_j^*\right\rangle &= -\hat{S}\eta_0 h_{eff,i} h_{eff,j}\hat{V}[\sin\theta(\sin\alpha_i\cos\alpha_j\sin(\varphi-\Omega_i)- \\ &\quad -\sin\alpha_j\cos\alpha_i\sin(\varphi-\Omega_j))+ \\ &\quad +\cos\theta\sin\alpha_i\sin\alpha_j(\sin(\varphi-\Omega_j)\cos(\varphi-\Omega_i)+ \\ &\quad +\sin(\varphi-\Omega_i)\cos(\varphi-\Omega_j))] \qquad (9)\end{aligned}$$

$h_{eff,i}$ and $h_{eff,j}$ are the magnitudes of the effective length vectors of antennas i and j, respectively, α and Ω are the polar angles describing the direction of the respective antenna, while θ and ϕ are the polar angles describing the direction of the incident wave. Since all three antennas can be combined at the SWAVES experiment, there are 9 equations for 6 unknown parameters. When the coordinate frame is chosen in a way that the effective length vector of one antenna points in the direction of one coordinate axis, say the Z antenna along the Z-axis, an analytical solution for the direction of the incident wave can be found.

$$\begin{aligned}\tan\varphi &= [\Im\left\langle V_X V_Z^*\right\rangle h_{eff,Y}\sin\alpha_Y\tan\Omega_Y\cos\Omega_Y- \\ &\quad -\Im\left\langle V_Y V_Z^*\right\rangle h_{eff,X}\sin\alpha_X\tan\Omega_X\cos\Omega_X]\times \\ &\quad \times[\Im\left\langle V_X V_Z^*\right\rangle h_{eff,Y}\sin\alpha_Y\cos\Omega_Y- \\ &\quad -\Im\left\langle V_Y V_Z^*\right\rangle h_{eff,X}\sin\alpha_X\cos\Omega_X]^{-1} \qquad (10)\end{aligned}$$

$$\begin{aligned}\tan\theta &= [\langle V_Z V_Z^*\rangle h_{eff,X}h_{eff,Y}\sin\alpha_X\sin\alpha_Y \\ &\quad \times(\cos(\varphi-\Omega_Y)\sin(\varphi-\Omega_X)- \\ &\quad -\cos(\varphi-\Omega_X)\sin(\varphi-\Omega_Y))] \\ &\quad \times[\Re\left\langle V_X V_Z^*\right\rangle\sin\alpha_Y\sin(\varphi-\Omega_Y)h_{eff,Y}h_{eff,Z} \\ &\quad -\Re\left\langle V_Y V_Z^*\right\rangle\sin\alpha_X\sin(\varphi-\Omega_X)h_{eff,X}h_{eff,Z} \\ &\quad +\left\langle V_Z V_Z^*\right\rangle h_{eff,X}h_{eff,Y} \\ &\quad \times(\cos\alpha_Y\sin\alpha_X\sin(\varphi-\Omega_X)- \\ &\quad -\cos\alpha_X\sin\alpha_Y\sin(\varphi-\Omega_Y))]^{-1} \qquad (11)\end{aligned}$$

A detailed derivation can be found in (*Oswald* [2005]). See also *Cecconi and Zarka* [2005] for the derivation of a similar equation with a slightly different coordinate frame. The solution for φ is not unambiguous, as one has to know the half sphere of the radio source in advance. It should be emphasized that not all available observables are used in these solutions, which results in loss of information. There exist numerical methods where this is avoided. For a general treatment of these possible methods see (*Oswald* [2005]). To compute the Stokes parameters once the direction is known, the method published in (*Cecconi and Zarka* [2005]) can be used. A matrix

equation is formed, which can be solved analytically. The equation, suitable for our coordinate frame is

$$\mathbf{Mx} = \mathbf{b} \tag{12}$$

with

$$\mathbf{b} = \begin{bmatrix} \frac{\langle V_X V_X^* \rangle}{\eta_0 h_{eff,X}^2} \\ \\ \frac{\langle V_Z V_Z^* \rangle}{\eta_0 h_{eff,Z}^2} \\ \\ \frac{\Re\langle V_X V_Z^* \rangle}{\eta_0 h_{eff,X} h_{eff,Z}} \\ \\ \frac{\Im\langle V_X V_Z^* \rangle}{\eta_0 h_{eff,X} h_{eff,Z}} \end{bmatrix} \tag{13}$$

$$\mathbf{x} = \begin{bmatrix} \hat{S} \\ \hat{S}\hat{Q} \\ \hat{S}\hat{U} \\ \hat{S}\hat{V} \end{bmatrix} \tag{14}$$

$$\mathbf{M} = \begin{bmatrix} M_{11} & M_{12} & M_{13} & 0 \\ M_{21} & M_{22} & M_{23} & 0 \\ M_{31} & M_{32} & M_{33} & 0 \\ 0 & 0 & 0 & M_{44} \end{bmatrix} \tag{15}$$

where

$$M_{11} = A_X^2 + B_X^2 \tag{16}$$
$$M_{21} = A_Z^2 + B_Z^2 \tag{17}$$
$$M_{31} = A_X A_Z + B_X B_Z \tag{18}$$
$$M_{12} = A_X^2 - B_X^2 \tag{19}$$
$$M_{22} = A_Z^2 - B_Z^2 \tag{20}$$
$$M_{32} = A_X A_Z - B_X B_Z \tag{21}$$
$$M_{13} = 2A_X B_X \tag{22}$$
$$M_{23} = 2A_Z B_Z \tag{23}$$
$$M_{33} = A_X B_Z + A_Z B_X \tag{24}$$
$$M_{44} = -(-A_X B_Z + A_Z B_X) \tag{25}$$

and

$$A_i = \cos\alpha_i \sin\theta - \sin\alpha_i \cos\theta \cos(\varphi - \Omega_i) \tag{26}$$
$$B_i = -\sin\alpha_i \sin(\varphi - \Omega_i) \tag{27}$$

Equation (12) is easily solvable, as long as **M** is not singular. This procedure has been successfully tested, using RPWS data from the Cassini

spacecraft. The important aspects of error analysis have been discussed on a theoretical base in (*Oswald* [2005]), as well as (*Oswald et al.* [2005]).

4. The numerical method to compute the effective length vectors

4.1. Calculation of the current distribution

The calculation has to be done in two steps. First the current distribution is computed by using the Method of Moments (MOM). Then, in a second step the effective length vectors are calculated.

The calculation of the current distribution on the surface of the spacecraft was done by using a modified version of the Antenna Scatterers Analysis Program (ASAP) which is an open source electromagnetic code. The surface of the spacecraft and the antennas were modeled as a wire grid which is excited by an electromotive force of 1V at the feeds of the antennas. So the electric field integral equations (EFIE) can be used to calculate the currents along the wires, which is a good approximation to the actual current distribution on the real spacecraft if the modeling is done properly.

$$\mathbf{E}(\mathrm{r}) = -\frac{v\eta}{4\pi k}\int_S G(\mathbf{r},\mathbf{r}')\mathbf{J}_s(\mathbf{r}')dS' \qquad (28)$$

$\mathbf{J}_S$ is the surface current density, $G(\mathbf{r},\mathbf{r}')$ is the Green function, η is the impedance of free space and k is the wave number. The surface integral over the surface of the spacecraft can be used because the whole spacecraft surface is made of conducting material.

This integral equation has to be solved in conjunction with the well known boundary conditions. The integral can be reduced to a scalar integral for the case of a cylindrical wire. Additionally the transverse currents on the wire are ignored and the currents are represented by single filaments along the wire axes. So the boundary conditions have to be satisfied only in axial direction.

The integral can be solved numerically by using the MOM which can be found in (*Harrington* [1968]). It is converted into a matrix equation which can be solved numerically. Hereby the currents along

each wire are represented as the sum of a set of two weighed sinusoidal base functions.

Once the current distribution is known, the input impedance can be computed by dividing the voltage at the feed by the current.

4.2. Calculations of the effective length vectors

The next step is the calculation of the effective length vectors. This can easily be achieved by integrating the retarded surface current density over the whole spacecraft and dividing it by the current at the antenna feed.

$$\mathbf{h}_{eff} = \frac{1}{I_0} \int_S \mathbf{J}_s(\mathbf{r}') e^{-\imath \mathbf{k}\cdot\mathbf{r}} dS' \tag{29}$$

I_0 is the current at the feed. Details can be found in (*Macher* [1997]).

5. The results of the determination of the effective length vectors of the STEREO/WAVES antennas

5.1. Introduction

Numerical calculations, using ASAP and the ASAP toolbox, to determine the characteristics of the three antennas of the STEREO/SWAVES experiment were performed. Such calculations were done fore the Cassini spacecraft (*Fischer et al.* [2001], *Fischer et al.* [2003] and *Vogl et al.* [2001]) as well as Mars Express (*Macher et al.* [2002] and *Macher et al.* [2004]) and other spacecraft in the past. A summary can be found in (*Rucker et al.* [2005]).

5.2. The spacecraft characteristics

One characteristic of the STEREO spacecraft is a certain degree of asymmetry. In contrast to many other spacecraft, the solar panels are positioned at different longitudinal distances at the spacecraft hull. Additionally the spacecraft consist of an about 6 meters long boom, and a turnable high gain antenna. These prominent features will have an influence on the antenna characteristics. The boom is divided into 4 sections with different diameters and has great influence upon the effective length vectors of the antennas.

The used, spacecraft fixed, reference frame is defined in a way to be spacecraft fixed with the positive

x-axis in a direction which will point to the sun during most of the time, so the antennas are mounted on the side of the hull which points to the negative x-axis. The solar panels point to the positive and negative y- axis and the z-axis is defined to complete the right handed cartesian frame (see figure 1).

For the description of the direction of the antennas we chose to use a spherical polar system which has the positive X-axis as polar axis. The angle ζ is the angle between the positive X-axis and the antenna, and ξ is the azimuthal angle around the X-axis, where antenna E1 is defined to have $\xi = 0$.

The direction of the boom defines the negative x-axis. There are 3 orthogonal monopole antennas, which are called E1, E2 and E3, each 6 meters long. They are directed about 125.26° from the x-axis and the difference in azimuth is 120°. The azimuth of antenna E1 defines the azimuth of 0°. It is expected, that the boom has an effect to push the 3 electrical antennas away from the boom's position. This effect is increased by the high gain antenna, which is located near the boom. The panels are expected to push the effective length vectors towards the negative x-axis.

The antennas will be directed away from the sun, so that they remain out of view of the sunward looking instruments on the spacecraft. Thus, the most interesting direction of incident waves is the positive x-axis.

The two spacecraft, A and B are almost identical, apart of some small differences of their instrumentation. The only difference which can be modeled within the limitations of ASAP is the second ring, mounted on the hull of spacecraft B on the positive x side, and not existent on spacecraft A.

With information about the base capacitances of antennas, coax cables and receivers, we were able to estimate and include the total base capacitances to be 90pF.

5.2.1. The model

The model of the Stereo spacecraft consist of the following parts:

1. The hull
2. 2 solar panels

3. The high gain antenna
4. Three 6 meter long antennas
5. A 6 meter long boom
6. A ring mounted on the hull of spacecraft A, two rings on spacecraft B

Size and position of the parts were measured from the relevant construction plans. The part of the tapered boom which is near to the spacecraft hull is modeled as prism with triangular base. Figures 3 shows the model from an oblique view.

5.3. The Computation

5.3.1. Computation of the effective length vectors

As a first step, we computed the currents at frequencies from 100 kHz to 16 MHz, with a spacing of 100 kHz, each frequency with 19 different angles of the HGA dish. This computation was performed by the ASAP program. Using this data, the impedances, admittances and effective length vectors can easily be computed with the toolbox devised at the Space Research Institute and updated to be suitable for the specific task of analyzing the antennas of SWAVES.

5.4. Calculations

Figure 4 shows a plot of the effective length vectors of spacecraft A, in relation to the physical antennas, which are represented in black. The frequency used for these plots is 500kHz, being well in the quasistatic regime. The direction of the incident wave is from the positive x-axis, simulating radiation from the sun.

Table 11 shows the results for all antennas on both spacecraft in tabulated form. The calculations were done for a frequency of 500 kHz and a HGA angle of 0 degrees. For comparison, the lengths and orientation information of the physical antennas are also added.

The quasistatic results were in full concurrence with our expectations. All electric antennas have lengths which are shorter than half the length of the physical antennas, as expected by theory for monopole antennas that are small in relation to the wavelength. The influence of the capacitances on the effective length vectors seems to be quite substantial. A similar calculation without taking the

capacitances into account resulted in effective length vectors which were approximately half the length of the physical antennas. Furthermore, it can clearly be seen that the solar panels push the electric antennas towards the negative x-axis with a counteracting influence of the boom. The difference between the two spacecraft, although not large, is definitely existent. It should be mentioned, however, that the radii of the antennas of the real spacecraft is not the same as the wire radius used for the calculations. This is a result of the limitations of the ASAP program. There could be a slight change of the magnitude of the effective length vectors due to this different radius. Further research on this matter will be done in future, mainly by using a different code for the current calculation, which allows different wire radii for different parts of the spacecraft.

5.4.1. Variation of the effective length vectors with frequency and direction

As mentioned before, direction finding is only possible in the lower frequency regions. At higher frequencies, the effective length vectors become complex and dependent on frequency and direction of incidence. The variability of the real part of the effective length vectors can be easily seen on figure 5. The plot was constructed by choosing 26 different directions and computing the effective length vectors for each frequency and each direction. The real part of all effective length vectors were plotted. The frequency is color coded. The imaginary parts of the vectors were ignored. The 26 sample directions were chosen to be the corners of a cube, and the midpoints of each area and each edge. The reason for the erratic behavior at high frequencies is the resonance at 14 MHz. Even though only the figures for spacecraft A are included, the plots of the antennas of spacecraft B show comparable results.

When direction finding is regarded to be possible with the knowledge of the directions of the electric antennas with an accuracy of 2 degrees, further analysis dictate an upper limit of not more than 2MHz where direction finding can be done by using standard methods. Fortunately further analysis shows that, even in the region near the resonance frequency, the effective length vectors behave in a predictable manner, i.e. they are not chaotic. Figure 6 shows the distance of the tip of the effective length vector of the E1 antenna from the quasistatic effective length vector in three dimensional complex space as

a function of direction of incidence at a frequency of 500 kHz.. It clearly can be seen that the function is continuous. The same is true for figure 7, although the variations are larger. This figure shows the result at 13.5 MHz, which is very near to the first resonance frequency. Further analysis shows that the function is also continuous regarding frequency variations.

5.4.2. Variation of the effective length vectors with frequency at fixed direction

The radiation to be measured by the spacecraft will have a direction of arrival roughly from the sun, which is located opposite to the boom (positive x-axis). Therefore it is useful to compute the geometry of the effective length vectors for this direction in detail. Figures 8 and 9 show the length of the effective length vectors as a function of frequency. Again, the result for STEREO A is plotted in solid lines while the results for STEREO B is plotted in dashed lines.

As one can see, the resonances at 14MHz change drastically the effective lengths of the antennas. The imaginary part of $\mathbf{h_{eff}}$ vanishes as the frequency goes to zero while the real part converges to the quasistatic limit.

5.4.3. Variation of the effective length vectors with different HGA angles

Analysis of the influence of the orientation of the HGA upon the effective length vectors has shown that the deviation is, in general, less then one degree at low frequencies. As an example, the coordinates of the effective length vector of E1 is shown in table 2. The frequency used to produce this data was 500kHz.

5.4.4. The impedances and admittances

On the plots of the admittances, the first resonances can be seen at a frequency between 13 and 14 MHz. A resonance exists, if the effective length of the antenna is equal to $\frac{1}{4}$ of the wavelength of the incident radiation. In the case of the spacecraft, the length of the distance between the tip of the antenna and the furthest point on the spacecraft represents half of the wavelength. In case of STEREO, the longest distances are between the boom and the antennas and between the edge of the opposite solar panel and the tip of the antennas. The wavelength of an electromagnetic wave at 12 MHz is 25 meters, so $\frac{\lambda}{4}$ is 6.25 m. Hence we would expect two resonances in the frequency range around 12MHz, but the in-

clusion of the capacitances of the receiver, the cable and the antenna mounting has the effect to decrease the resonance frequency. When regarding the case of transmitting antennas, the base capacitances are parallel to the antenna capacitances and both can be added. To get the overall impedance, the reciprocal values have to be added, while the admittances have simply to be added. The two resonances can partly be seen on the plot of the admittances, but in general they are too close together to be resolved.

One example of the resultant impedance can be seen in Figures 10 and 11. While in the first plot, the real and imaginary parts are plotted as a function of frequency, the imaginary part is plotted as a function of the real part in the lower graph. The resonance occurs when the imaginary part of the impedance is zero. Then the antenna is pure resistive. It can clearly be seen in the plots.

6. Conclusion

The NASA mission STEREO will provide new insights into the physics of the solar system by using stereoscopic methods to analyze radio sources. It has been shown that the method relies on direction finding, of which a short overview was given in section 3. It was also shown that direction finding relies heavily upon a detailed knowledge of the receiving properties of the antennas, which can be represented by a single entity, the effective length vector. A numerical method was used to compute the effective length vectors of the antennas of the STEREO spacecraft.

Acknowledgments. (Text here)

References

Cecconi, B., and P. Zarka (2004), Direction finding and antenna calibration through analytical inversion of radio measurements performed using a system of 2 or 3 electric dipole wire antennas on a 3 axes stabelized spacecraft, *Radio Sci.*, *40*, RS3003, doi:10.1029/2004RS003070.

Fischer, G., W. Macher, H. Rucker, H. Ladreiter, and D. Vogl (2001), Wire-grid modeling of Cassini spacecraft for the determination of effective antenna length vectors of the RPWS antennas, in *Proc. Planetary Radio Emissions V*, edited by H. Rucker, M. Kaiser, and Y. Leblanc, pp. 347–356, Austrian Academy of Sciences Press, Vienna.

Fischer, G., W. Macher, H. Rucker, H. Ladreiter, and D. Vogl (2003), Reception properties of the

Cassini/RPWS antennas from 1 to 16 mhz, poster at the EGS-AGU-EUG Joint Assembly, Nice.

Harrington, R. (1968), *Field Computation by Moment Methods*, Robert E. Krieger Publishing Company.

Macher, W. (1997), Theorie effektiver hoehenvektoren von antennen mit anwendung auf das radio and plasma wave science experiment der Cassini raumsonde, Diploma thesis, Graz University of Technology.

Macher, W., B. Schrausser, G. Fischer, H. Rucker, H. Lammer, C. Kolb, and G. Kargl (2002), Analysis of sounding antennas of the mars-express marsis experiment, in *Proc. 2nd European Workshop on Exo/Astrobiology*, edited by H. Sawaya-Lacoste, pp. 539–540, ESA Publications Division, Noordwijk, ESA SP-518.

Macher, W., H. Rucker, G. Fischer, and M. Team (2004), Analysis of the marsis antenna system onboard mars express, poster at the EGU 1st General Assembly, Nice.

Oswald, T.H. (2005), Electromagnetic waves in space and the stereo/waves experiment, Master's thesis, University of Graz.

Oswald, T., H. Rucker, W. Macher, G.Fischer, and U. Taubenschuss (2005b), Direction finding, *Technical Report of the Space Research Institute/Austrian Academy of Science, Nr. 168.*

Rucker, H. O., W. Macher, and S. Albrecht (1997), Experimental and theoretical investigations on the Cassini RPWS antennas, in *Proc. Planetary Radio Emissions IV*, edited by H. Rucker, S. J. Bauer, and A. Lecacheux, pp. 327–337, Austrian Academy of Sciences Press Vienna.

Rucker, H., W. Macher, G. Fischer, T. Oswald, J.-L. Bougeret, M. Kaiser, and K. Goetz (2005), Analysis of spacecraft antenna systems: Implications for stereo/waves, *Adv. Space Res.*,*36*,1530-1533, doi: 10.1016/j.asr.2005.07.060.

Vogl, D., H. Ladreiter, P. Zarka, H. Rucker, W. Macher, W. S. Kurth, D. Gurnett, and G. Fischer (2001), First results on the calibration of the Cassini RPWS antenna system., in *Proc. Planetary Radio Emissions V*, edited by H. Rucker, M. Kaiser, and Y. Leblanc, pp. 357–366, Austrian Academy of Sciences Press, Vienna.

Vogl, D., et al. (2004), In-flight calibration of the Cassini/RPWS antenna system for direction finding and polarization measurements, *J. Geophys. Res.*, *109*, A09S17, doi:10.1029/2003JA010261.

T.H. OSWALD, Space Research Institute, Schmiedlstrasse 6, Graz, A-8042, Austria. (thomas.oswald@oeaw.ac.at)

(Received _____.)

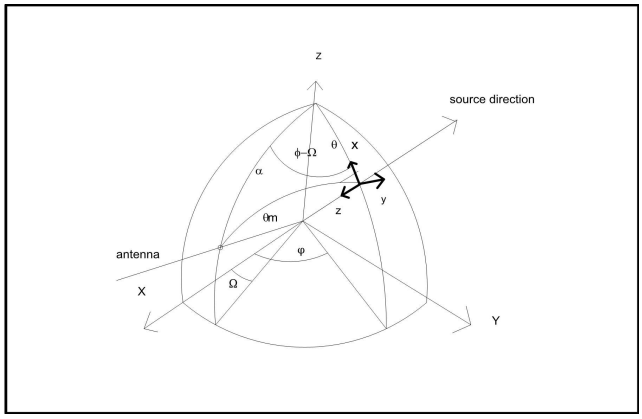

Figure 1. Relation between wave frame and spacecraft frame

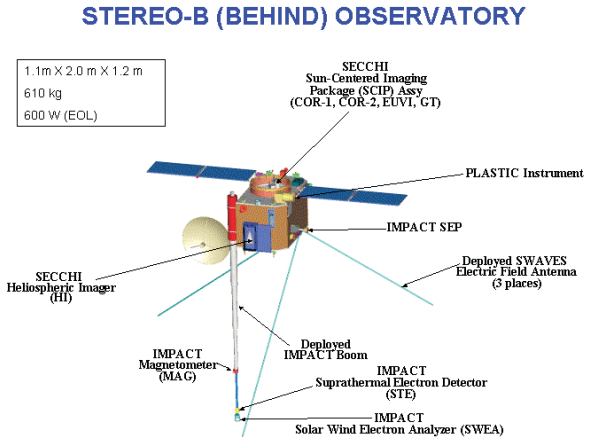

Figure 2. Artist's view of STEREO B spacecraft, with permission of NASA

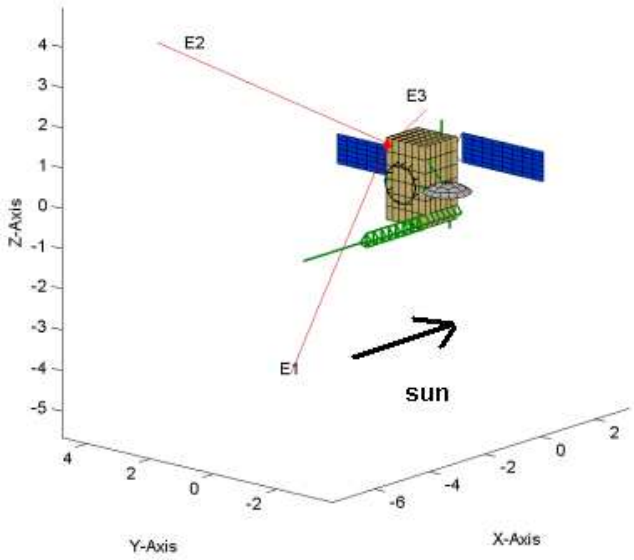

Figure 3. STEREO A

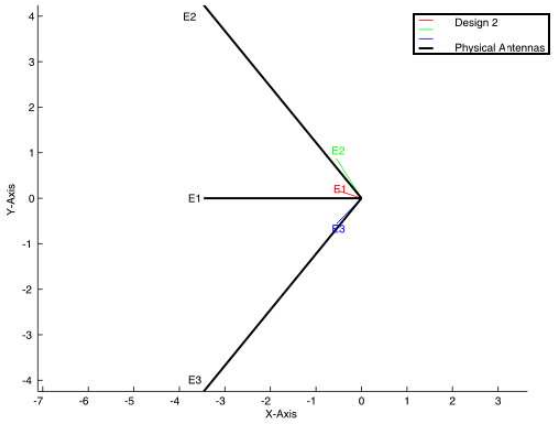

Figure 4. STEREO A: Effective Length Vectors

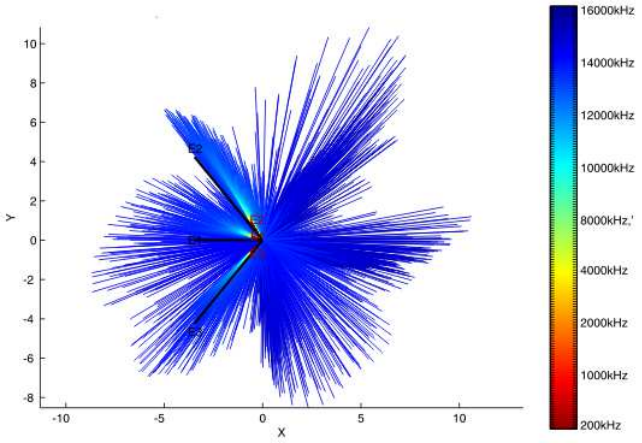

Figure 5. The spatial distribution of the real parts of the effective length vectors of STEREO A with a frequency up to 16MHz

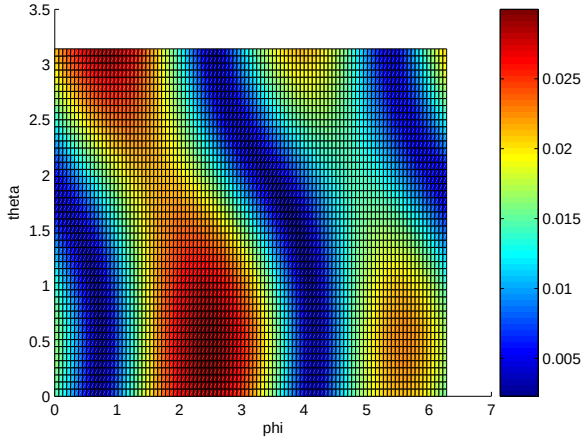

Figure 6. The difference between the quasistatic effective length vector and the effective length vector in three dimensional complex space at 500kHz as function of direction of incidence.

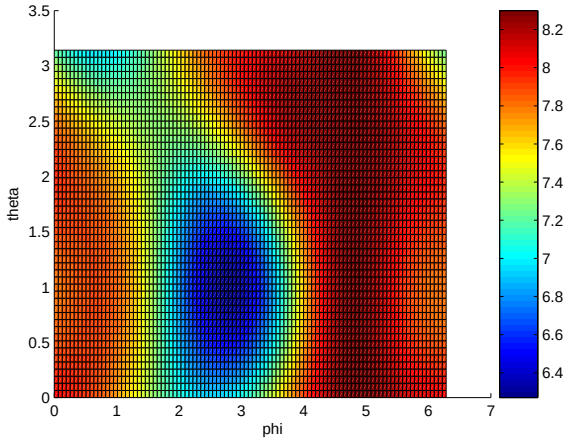

Figure 7. The difference between the quasistatic effective length vector and the effective length vector in three dimensional complex space at 13.5MHz as function of direction of incidence.

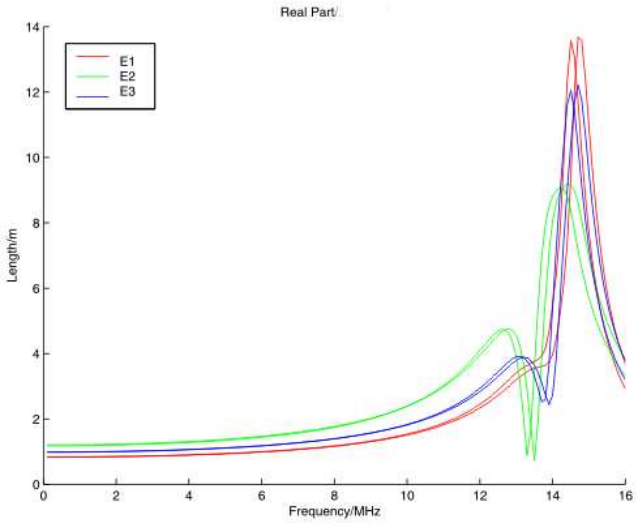

Figure 8. The length of the real parts of the electric antennas of STEREO A

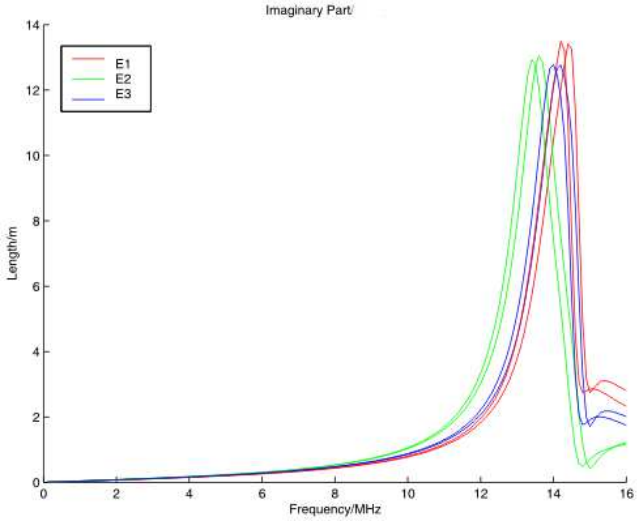

Figure 9. The length of the imaginary parts of the electric antennas of STEREO A

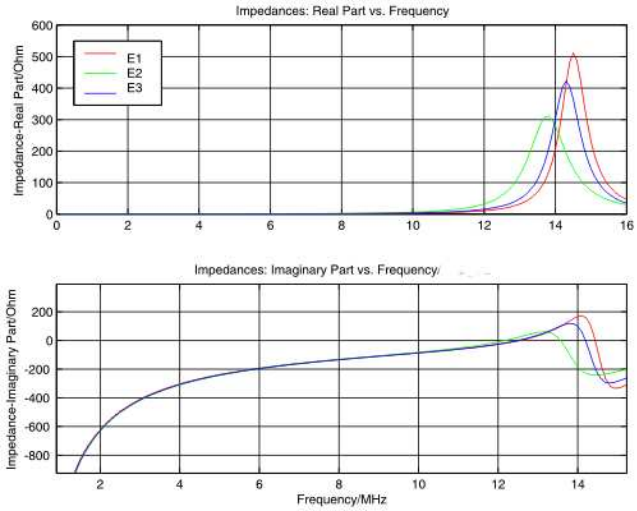

Figure 10. Impedances of STEREO A

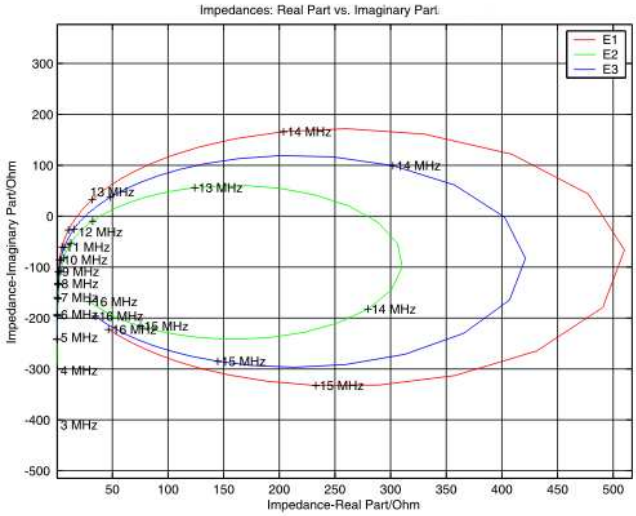

Figure 11. Impedances of STEREO A

Table 1. Effective length vectors at 500kHz

		STEREO A	STEREO B	Physical antennas
E1	Length/m	0.83	0.84	6.00
	ζ/°	128.3	127.2	125.26
	ξ/°	15.0	13.3	0.0
E2	Length/m	1.21	1.18	6.00
	ζ/°	117.1	117.4	125.26
	ξ/°	125.8	125.2	120.0
E3	Length/m	0.99	0.98	6.00
	ζ/°	123.5	123.3	125.26
	ξ/°	-137.2	-135.4	-120.0

Table 2. Variation of E1 due to HGA angle variation of STEREO A at 500kHz

HGA angle	h_{eff}	ζ	ξ
-90	0.83	128.5	14.5
-80	0.83	128.5	14.5
-70	0.83	128.5	14.4
-60	0.83	128.4	14.5
-50	0.83	128.4	14.5
-40	0.83	128.4	14.5
-30	0.83	128.4	14.2
-20	0.83	128.3	14.7
-10	0.83	128.3	14.9
0	0.83	128.2	15.0
10	0.83	128.1	15.0
20	0.83	128.0	15.1
30	0.83	127.8	15.1
40	0.83	127.7	15.2
50	0.83	127.7	15.2
60	0.83	127.6	15.3
70	0.83	127.6	15.3
80	0.83	127.7	15.4
90	0.83	127.7	15.4